# The Appearance of the Warburg Effect in the Developing Avian Eye Characterized In Ovo: How Neurogenesis Can Remodel Neuroenergetics

Antoine Cherix,[1] Laurent Brodier,[2,3] Carole Poitry-Yamate,[1] Jean-Marc Matter,[2,3] and Rolf Gruetter[1]

[1]Laboratory for Functional and Metabolic Imaging, École Polytechnique Fédérale de Lausanne, Lausanne, Switzerland
[2]Department of Molecular Biology, Sciences III, Université de Genève, Geneva, Switzerland
[3]Department of Biochemistry, Sciences II, Université de Genève, Geneva, Switzerland

Correspondence: Antoine Cherix, Wellcome Centre for Integrative Neuroimaging, FMRIB, Nuffield Department of Clinical Neurosciences, University of Oxford, Oxford, UK; antoine.cherix@ndcn.ox.ac.uk. Jean-Marc Matter, Department of Molecular Biology and Department of Biochemistry, Sciences III, 30, quai Ernest-Ansermet, 1211 Genève 4, Switzerland; jean-marc.matter@unige.ch.

AC and LB contributed equally. JMM and RG share senior authorship.

**Received:** November 15, 2019
**Accepted:** March 9, 2020
**Published:** May 11, 2020

Citation: Cherix A, Brodier L, Poitry-Yamate C, Matter J-M, Gruetter R. The appearance of the Warburg effect in the developing avian eye characterized in ovo: how neurogenesis can remodel neuroenergetics. *Invest Ophthalmol Vis Sci*. 2020;61(5):3. https://doi.org/10.1167/iovs.61.5.3

**Purpose.** The avian eye is an established model for exploring mechanisms that coordinate morphogenesis and metabolism during embryonic development. Less is known, however, about trafficking of bioenergetic and metabolic signaling molecules that are involved in retinal neurogenesis.

**Methods.** Here we tested whether the known 3-day delayed neurogenesis occurring in the pigeon compared with the chick was associated with a deferred reshaping of eye metabolism in vivo. Developmental metabolic remodeling was explored using $^{1}$H-magnetic resonance spectroscopy of the whole eye and vitreous body, in ovo, in parallel with biochemical and molecular analyses of retinal, vitreous, and lens extracts from bird embryos.

**Results.** Cross-species comparisons enabled us to show that a major glycolytic switch in the retina is related to neurogenesis rather than to eye growth. We further show that the temporal emergence of an interlocking regulatory cascade controlling retinal oxidative phosphorylation and glycolysis results in the exchange of lactate and citrate between the retina and vitreous.

**Conclusions.** Our results point to the vitreous as a reservoir and buffer of energy metabolites that provides trophic support to oxidative neurons, such as retinal ganglion cells, in early development. Through its control of key glycolytic regulatory enzymes, citrate, exchanged between extracellular and intracellular compartments between the retina and vitreous, is a key metabolite in the initiation of a glycolytic switch.

Keywords: retina, metabolic switch, neurogenesis, retinal ganglion cell, mitochondria, lactate, citrate, phosphofructokinase, metabolism, chick, pigeon

Cellular metabolism is influenced by factors such as oxygen and energy substrate availability and is tightly controlled in response to the cell microenvironment. This is the case during embryogenesis, when the cellular environment undergoes dynamic changes as tissues grow and organize, and as cells proliferate and differentiate, implicating profound remodeling of metabolic pathways that control the fine-tuning between anabolic and catabolic processes. The avian embryo, and its eye in particular, have historically proven to be an accessible and well-established model for investigating mechanisms that coordinate neurogenesis. However, the associated metabolic-related mechanisms have yet to be explored experimentally in the avian eye in ovo.

Healthy mature cells rely on glucose metabolism and mitochondrial oxidative phosphorylation in the presence of oxygen. Under limited oxygen availability, cells switch to anaerobic glycolysis (Pasteur effect), the pathway that converts glucose to lactate. Aerobic glycolysis (Warburg effect), however, refers to the cellular conversion of glucose to lactate, regardless of oxygen conditions, emphasizing a metabolic choice that is not constrained by the lack of oxygen. Although aerobic glycolysis is often associated with supporting cell proliferation and malignant cells,[1–3] a host of recent studies (see, Jones[4]) indicate that it can be a metabolic choice of adult tissues. One prime example is the adult retina, a tissue known for its exceptionally high rate of aerobic glycolysis, as originally observed in the rat by Warburg[3] and in the chick and pigeon by Krebs.[5]

Enzyme histochemistry and immunohistochemistry measurements demonstrated that the developing chick retina undergoes progressive spatial segregation of mitochondria, progressive loss of mitochondrial enzymes from the inner retina (thereby decreased respiratory capacity), and concomitant increases in the expression of the M

isoform of lactate dehydrogenase (LDH) (associated with anaerobic metabolism) in regions of low oxidative capacity.[6–8] These findings raise two important questions: (1) Is this enzymatic remodeling associated with a change in metabolite content; and (2) Does this process relate to neurogenesis and/or retinal ganglion cell (RGC) axogenesis?[9]

In recent magnetic resonance studies, eggs of live chick embryos were imaged using magnetic resonance imaging at 7T to characterize the entire embryonic tissue structurally and anatomically at different developmental stages[10] through to hatching.[11] With a focus on the avian eye, we take these studies a step further to characterize how energy metabolism (i.e., glycolytic and oxidative intermediates and/or products) is associated with structure and compartmentation during the time window of retinal neurogenesis using in vivo $^{1}$H-magnetic resonance spectroscopy ($^{1}$H-MRS) at ultra-high magnetic field. We capitalized on the fact that both chick and pigeon retinas grow at a similar pace; yet, cell differentiation and the production of RGCs are delayed by approximately 3 days in the pigeon,[12] providing a strategy to directly link our MRS measurements to metabolic adaptations taking place during neurogenesis.

Using a multimodal approach of $^{1}$H-MRS combined with molecular and biochemical analyses, we report the emergence of a developmental glycolytic switch linked to retinal neurogenesis. We show that RGC axogenesis and their axonal accumulation of mitochondria that create the need to fuel mitochondrial oxidative metabolism coincide temporally with the disappearance of citrate and with a pH rise in the neighboring vitreous compartment. These changes appear to serve a metabolic signaling function in a cascade that involves phosphofructokinase 2 (PFK2) and pyruvate dehydrogenase kinase (PDK), leading to aerobic glycolysis activation in the retina. This results in the net accumulation of vitreous lactate, a recognized retinal energy source in chick embryo eyes.[13]

## Materials and Methods

### Experimental Design

Chick embryos (unknown sex) from White Leghorn strain (UNIGE Animal Resources Center, Geneva, Switzerland) were staged according to Hamburger and Hamilton.[14] Fertilized pigeon eggs were supplied by Philippe Delaunay (Pigeonneau de la Suisse Normande, Croisilles, France). Experimental procedures were carried out in adherence with the ARVO Statement for the Use of Animals in Ophthalmic and Vision Research and in accordance with Federal Swiss Veterinary Regulations. Bird eggs were hatched in a portable incubator keeping humidity and temperature (37°C) of the ambient air at optimal conditions for embryo development.[12] A group of six animals were scanned longitudinally in the MRS experiments, and all other experiments were performed on individual groups described in each section. Because of the technical constraints of $^{1}$H-MRS, focus was put on the embryonic stages E6 and E8 for the in vivo measurements to reflect the peak in RGC production in the chick occurring at day 6.[12] A detailed description of the Materials and Methods used can be found in the Supplementary Material. Statistical analyses are explained in the Supplementary Material and in the figure legends.

## Results

### Mitochondrial Oxidative Metabolism Decreases During Retinal Development

To determine the temporal pattern of oxidative metabolism and its relationship to mitochondrial biogenesis, content and function in the embryonic retina, we first examined total retinal mitochondrial mass, assessed by quantifying mitochondrial DNA (mt-DNA) copy number in the chick and pigeon from E3 to E15. The results are shown in Figure 1A with the following observations: (1) mitochondrial content was the highest at the early embryonic stages; and (2) it gradually decreased from E3 to E10 (Fig. 1A). This decrease coincided with a decrease in the expression of the master regulator of mitochondrial biogenesis peroxisome proliferator-activated receptor gamma coactivator 1 (PGC1)$\beta$, whereas PGC1$\alpha$ slightly decreased in the pigeon and increased in the chick (Fig. 1B). Many other genes control and regulate the mitochondrial content and function, and as such, the expression of nuclear respiratory factor (Nrf), mitochondrial transcription factor A (Tfam), nuclear receptor corepressor 1 (Ncor1), and Nip3-like protein X (Nix)[15–18] have been investigated (Fig. 1C). The drop in relative Nrf and Tfam mRNA content were consistent with lower mitochondrial biogenesis. The increase in Ncor1 also supports the idea that mitochondria biogenesis is repressed, whereas the steady levels of Nix is evidence against a mitophagy-related process. Retinal progenitor cells have a fast cell cycle[19] that lasts ~12 hours, and cytokinesis is a contributing factor to mitochondrial decrease. Although cell number increases by approximately 100-fold between E4 and E8,[12] the approximate four-fold decrease of mt-DNA content during the same period remains relatively modest in comparison, an indication that active mitochondria production keeps pace relatively well with the rapid cell division.

Retina were transfected with a CMV-GFP reporter together with an ubiquitous mitochondria-targeted label (CMV-mitoDsRed2), whose accumulation in mitochondria has been shown to depend on mitochondrial membrane potential.[20] Results indicated a drop of mitochondrial activity (Fig. 1D), which in the pigeon was delayed by ~3 days, suggesting that the temporal pattern of mitochondrial activity, unlike mitochondrial mass, is related to neurogenesis. Quantitative analysis of the relative mt-DNA copy number in committed RGCs expressing the bHLH transcription factor Atonal homolog 7 (Atoh7) at high level (Atoh7-RFP; Fig. 1E), confirmed that the high content of mitochondria was comparable to that in early progenitors (not significant [n.s.]). This was corroborated by the high level of mitochondria activity in newborn RGCs identified with a Chrnb3-GFP (Cholinergic Receptor Nicotinic Beta 3 Subunit) reporter (Fig. 1F).[20]

To assess mitochondrial activity in newly differentiated RGCs, confocal, time-lapse imaging, and kymograph analysis of outgrowing axons were performed 24 hours after electroporation of E5 retinas with Chrnb3-GFP, CMV-GFP, and CMV-MitoDsRed2 plasmids. The results shown in Figures 1G through 1J indicate that active mitochondria, located in the RGC axons (Fig. 1G), are particularly prominent in the area of growth cone expansion (Fig. 1H), with a significant anterograde directionality (Figs. 1I, 1J).

Finally, under the experimental conditions used in our study, an examination of the high-resolution proton nuclear magnetic resonance ($^{1}$H-NMR) spectroscopic 1.28 ppm resonance signal obtained from E6 and E8 retinal extracts inde-

Investigative Ophthalmology & Visual Science

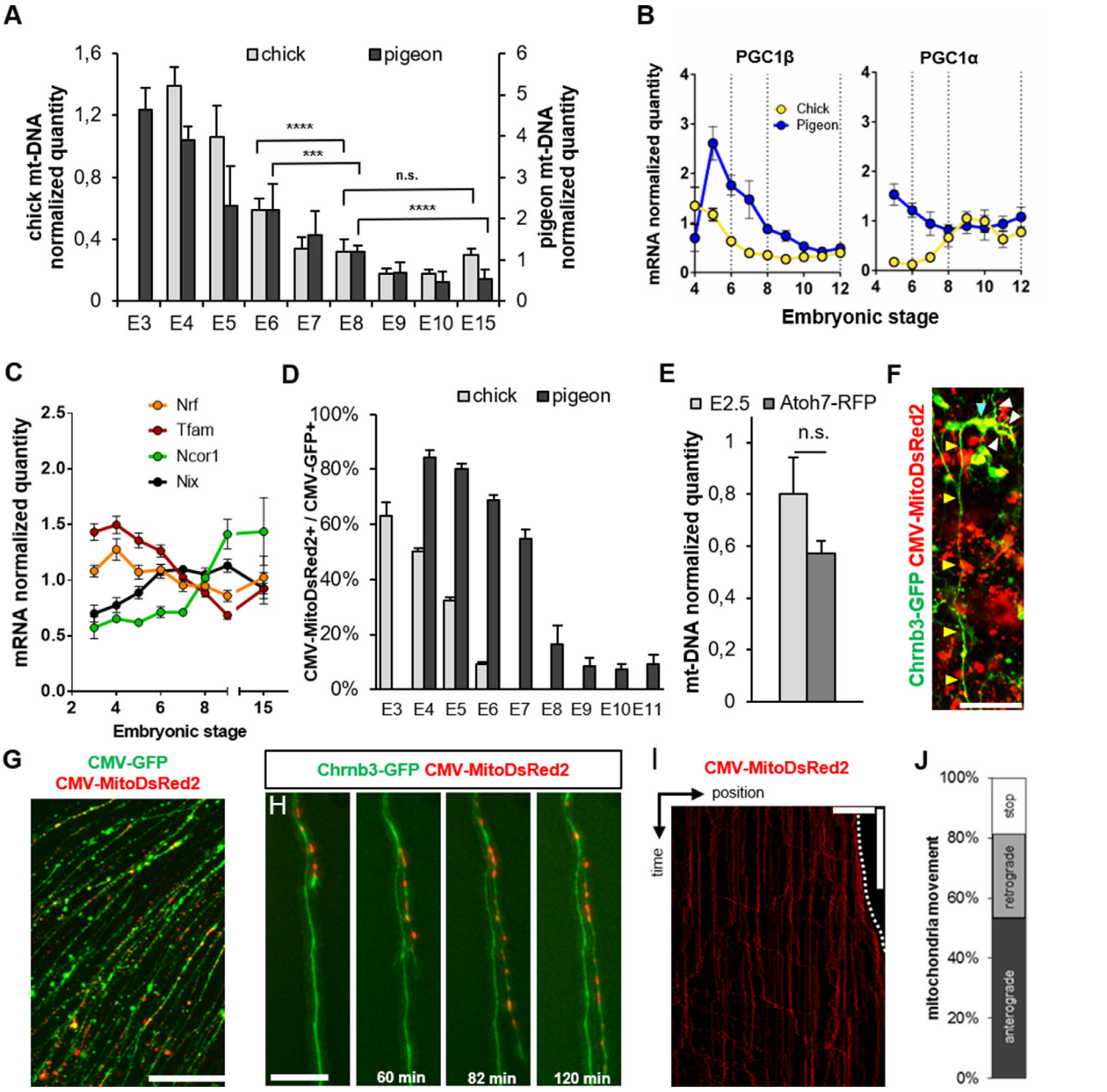


**Figure 1.** Mitochondrial oxidative metabolism decreases during retinal development. (**A**) Ratio ± SD of mt-DNA to g-DNA in whole retinas isolated from embryonic chick and pigeon. Data are from biological triplicates with four targets (chick) or two targets on mt-DNA (pigeon). Chick E6 versus E8, $^{****}P < 0.0001$, E8 versus E15, $P = 0.40$; [n.s.] not significant, pigeon E6 versus E8, $^{***}P = 0.0002$, E8 versus E15, $^{****}P < 0.0001$; unpaired Student's *t*-test. (**B**) Relative mRNA expression of the master mitochondrial biogenesis factor PGC1 in chick and in pigeon retina. PGC1$\beta$ was decreased over time (time effect: $F_{8,36} = 19.95$, $P < 0.0001$) with a 3-day delay between pigeon and chick (interaction: $F_{8,36} = 47.11$, $P < 0.0001$; 2-way ANOVA). PGC1$\alpha$ expression was time-dependent as well (time effect: $F_{7,32} = 4.03$, $P = 0.002$) with a different pattern between pigeon and chick (interaction: $F_{7,32}$=17.29, $P < 0.0001$; 2-way ANOVA). (**C**) Relative mRNA expression in chick retina from different target genes involved in mitochondrial biogenesis and autophagy. Between E6 and E8 a drop in Nrf (–13%; $P = 0.049$) and Tfam (–30%; $P < 0.0001$) is observed together with an increase in Ncor1 (+44%; $P < 0.0001$), whereas no difference was observed in Nix (n.s.); unpaired Student's *t*-test. At each developmental stage, data are from three biological replicates, including 3 to 10 retinas, and presented as mean ± SD. (**D**) Proportion ± SD of cells that contain MitoDsRed2-labeled mitochondria during development of the chick and pigeon retinas, including 3 to 10 pooled retinas for each condition, and processed as one biological replicate. All pairwise comparisons give $P < 0.001$, except between pigeon E8 and E9 in which $P < 0.05$, and between E9, E10, and E11 in which the differences are nonsignificant ($\chi^2$ test; chick E3 n = 370 cells, E4 n = 9754, E5 n = 8480, E6 n = 4109; pigeon E4 n = 827, E5 n = 4861, E6 n = 3808, E7 n = 2516, E8 n = 338, E9 n = 131, E10 n = 55, E11 n = 118). (**E**) Mitochondrial content in whole E2.5 (HH18) chick retina and in a subset of chick committed and newborn RGCs identified with Atoh7-RFP and selected by Fluorescence-activated cell sorting (FACS) (unpaired *t*-test; $P = 0.134$; n.s., $n = 3$). (**F–J**) E5 chick retinas were coelectroporated with CMV-GFP and CMV-MitoDsRed2 (**G**), or Chrnb3-GFP and CMV-MitoDsRed2 (**F, H, I, J**) and observed 24 hours later. (**F**) The soma (*cyan arrowhead*), the dendrites (*white arrowheads*), and the axon (*yellow arrowheads*) of a single RGC by confocal imaging. (**G**) Axons growing on the basal surface by confocal imaging. (**H**) Stills from a time-lapse movie in the red and green channels, showing growth cone progression and mitochondria dynamics. (**I**) A kymograph of spatial position of mitochondria in a growing RGC axon. The vertical axis represents time at 30 second intervals. The *dotted line* indicates position of the growth cone. (**J**) Proportion of mobile mitochondria moving in the anterograde or retrograde direction and stopped mitochondria from kymograph presented in **I**. *Scale bars*: 50 µm (**F** and **I** horizontal); 100 µm (**G**); 30 µm (**H**); 1800 seconds (**I** vertical).

Investigative Ophthalmology & Visual Science

pendently confirmed the established delay in the onset of neurogenesis in pigeon retina, relative to that in the chick (Supplementary Fig. S1A). This signal corresponds to the lipid methylene resonance, a proposed marker of neural progenitor cells (NPCs),[21] which has been associated with apoptosis, appearance of mobile lipid droplets,[22] and high density of actively dividing cells.[23] Normalization of the 1.28 ppm peak using either the ubiquitous cell marker creatine, or the neuron cell marker N-acetyl-aspartate, led to the following observations: (1) both chick and pigeon retinas displayed a comparable reduction in the ratio of NPC marker to total cell population; and (2) the ratio of NPCs to the total neuronal population was two-fold lower in the chick at E8 than in the pigeon, confirming a lower level of neuronal differentiation in the pigeon at this stage.

Together these results indicate that (1) mitochondrial content, activity, and biogenesis all decrease in the retina during the first week of embryonic development; (2) whereas mitochondrial activity declines globally in the retina, it remains stable in the RGCs; and (3) the reduction of mitochondrial activity is delayed by 3 days in pigeon retina relative to that in the chick.

## The Time Window of Retinal Mitochondrial Oxidative Metabolism Decrease Coincides With a Change in the Profile of Lactate of the Whole Eye, but not of the Retina

Because energy metabolism reflects structure and function, and because other components of the eye might benefit and/or assist the metabolic remodeling, we sought to assess whether the aforementioned spatial redistribution of RGC mitochondria is accompanied by detectable differences in energy metabolite concentrations between the whole eye and the isolated retina. For this, a conventional neurochemical profile using in vivo $^{1}$H-MRS was acquired (Figs. 2A–D).

The whole eye of chick and pigeon embryos (Fig. 2A) were individually scanned at E6 and rescanned at E8 at 14.1 Tesla. The resulting $^{1}$H-MRS spectra are shown in Figures 2B and 2C. As described in Materials and Methods, embryos at stage E8 were scanned ex ovo, that is, the embryo was bathed in cold saline buffer to minimize spontaneous muscular contraction in ovo. Because of the difference in lactate content of the whole eye bathed in saline milieu and an extra-embryonic milieu (Fig. 2D), relative comparisons were made between species at a given embryonic stage (see Supplementary Methods). Using this approach, we found a higher content of whole eye lactate at E8 in the chick compared with the pigeon (+72 ± 20%, $P = 0.004$) (Fig. 2B). In contrast, the metabolic profile of the isolated retina (Supplementary Figs. S1B, S1C) indicated that lactate did not rise in the avian retina (Fig. 2E) between E6 and E8.

## A Transient Net Accumulation of Vitreous Lactate Marks the Appearance of a Retina Metabolic Switch, With a Delayed Onset in the Pigeon

The vitreous is a potential reservoir of energy metabolites for the retina and a channel for the movement of metabolites within the eye. To determine whether the measured lactate in the whole eye originates from this compartment, MRS scans were performed with the acquisition voxel positioned over the vitreous (Fig. 3A, top panel), the largest ocular compartment by volume. The resulting metabolic profiles (Fig. 3A, lower panel) consisted mainly in water-soluble energy-related metabolites, such as lactate, glucose, and citrate. Quantification of the spectra at E6 and E8 revealed a two-fold increase of lactate in chick vitreous (+106 ± 30%, $P = 0.004$), whereas no apparent difference in pigeon embryos was observed (n.s.; Fig. 3B). The reliability of these in vivo measurements was confirmed by high-resolution $^{1}$H-NMR using isolated vitreous extracts (Figs. 3C, 3D). In the pigeon, lactate content peaks in the vitreous at E12 (Fig. 3D), in line with the ~3-day delay decline in retinal mitochondrial function (Fig. 1D). As such, the net accumulation of lactate in the vitreous appears to be developmentally controlled in the avian retina and underlies a metabolic switch. Of note, lactate increase in vitreous is transient in nature, given the drop occurring at E15 in the chick (–40%; $P = 0.002$) and in the pigeon (–84%; $P = 0.00012$) after an apparent maximum (i.e., at E8 for chick and E12 for pigeon; Fig. 3D). It is noteworthy that lactate in the isolated chick lens increased only from E8 onward (Supplementary Fig. S1D).

## A Decrease in Vitreous Citrate Parallels Lactate and pH Increases as the Retina Undergoes a Metabolic Switch

The vitreous is considered inert, and a shock-absorbing tissue,[24] and although it plays a major role in vision, it is also implicated in ocular diseases.[25,26] The latter finding suggests that the vitreous may play a more significant role, functionally and/or metabolically, than previously thought. For this reason, we further characterized our MRS spectra from chick E6 and E8 embryos, with particular attention to citrate, originally detected in vivo (Fig. 3A). Citrate contains three carboxylic acids, and its chemical shift (resonance from four methylene protons) is thus highly pH sensitive.[27] Based on the identification of vitreous citrate at 2.6 ppm (Fig. 4A), we asked whether an associated pH change was measurable in vivo. As shown in Figures 4B and 4C, with citrate as an internal probe, we observed a difference of +0.26 ± 0.11 pH units ($P = 0.04$) between chick vitreous at E6 and E8. This difference corresponds to a ~1.8-fold drop in proton concentration. Consistent with a delayed metabolic switch in the pigeon, the pH of pigeon vitreous at E8 was comparable to that in the chick at E6. Interestingly, the drop in proton concentration was associated with an approximate two-fold drop in citrate in chick vitreous in vivo (Fig. 4D; –51 ± 27%; $P = 0.044$), and vitreous pH appeared to be related to the citrate to lactate ratio (Fig. 4E). Because quantification of vitreous metabolites other than lactate in vivo led to higher fitting errors (Cramér-Rao Lower Bound (CRLB): glucose, 32.4 ± 4.3%; citrate, 33.0 ± 4.8%), high-resolution $^{1}$H-NMR spectroscopy was used to confirm citrate content changes from samples of isolated vitreous (Figs. 4F, 4G). Citrate quantification in these extracts also indicated a drop between E6 and E8 in the chick vitreous (–77 ± 32%; $P = 0.012$), and moreover confirmed a 3-day delay in the pigeon (–55 ± 17%; E8 vs. E12; $P = 0.005$). Interestingly, an increase in a singlet resonance in Figure 4F, which we assigned to oxaloacetate (OAA), a by-product of citrate metabolism, displayed dynamics similar to that of lactate: OAA tend to increase between E6 and E8 in chick extracts (Supplementary Fig. S1E; +72 ± 44%; $P = 0.084$); this increase was delayed in the pigeon by 3 days (+261 ± 56%, $P = 0.0001$), strengthening the link between metabolic remodeling and retinal neurogenesis in the avian eye. Although the ~5 mM lactate rise

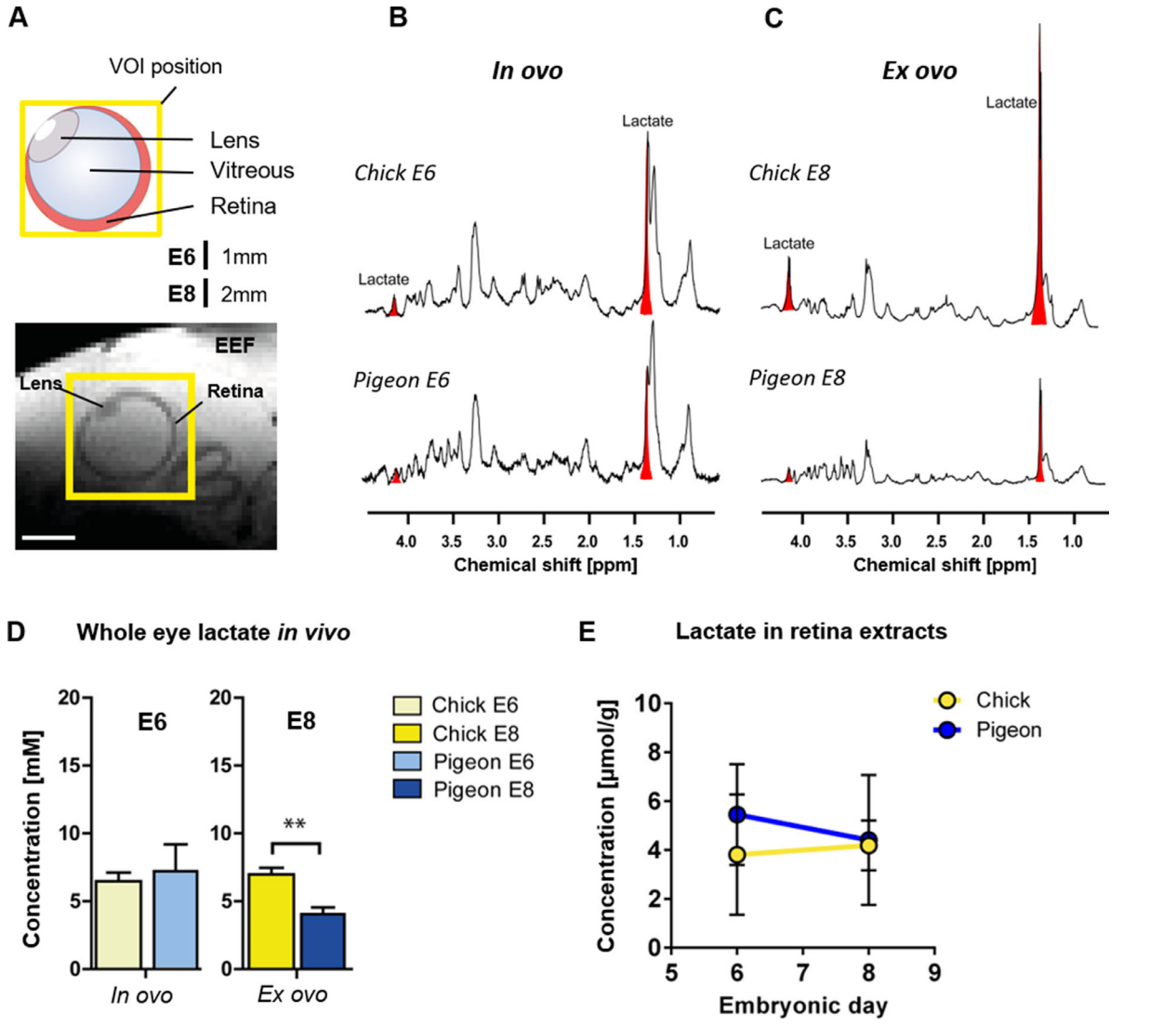


**Figure 2.** The time window of retinal mitochondrial oxidative metabolism decrease coincides with a change in the profile of lactate of the whole eye, but not of the retina. (**A**) Localized in vivo $^{1}$H-MRS of avian embryo eye. (**A**, *top*) Schematic representation of the volume-of-interest (VOI; *yellow square*) position used for in vivo MRS and eye components with scale bars reflecting the chick eye dimensions at E6 and E8. (**A**, *bottom*) $T_2$-weighted magnetic resonance image of a chick eye at embryonic stage E6 with the position of the VOI (*yellow square*) for localized $^{1}$H-MRS. *Scale bar*: 2 mm. (**B–C**) In vivo spectra acquired for lactate quantification in the whole eye. The VOI selected for acquisition surrounded the whole eye, and the inclusion of extraembryonic fluid (EEF) at E6 (**B**; in ovo scan) or PBS medium at E8 (**C**; ex ovo scan) lead to visible partial volume effects, that is, incorporation of unwanted tissue in the VOI. As a result, the reported spectrum is the averaged signal of all included tissues. The sum of all the spectra per group is shown. Further details on spectrum labeling and fitting are shown in Supplementary Figure S3C. (**D**) Lactate concentration in the whole eye in vivo, quantified from in ovo spectra at E6 and ex ovo spectra at E8 (mean ± SEM, unpaired Student's *t*-test, $^{**}P < 0.005$, $n = 5$–6 per group). Because of the high CRLB of other metabolites, results are mainly indicative and reported in Supplementary Figures S1C, S1D. (**E**) Lactate concentration in the retina quantified from the high-resolution $^{1}$H-NMR spectra of metabolite extracts (mean ± SEM, $n = 6$–8 per group).

seems unlikely to be the anaplerotic consequence of the more modest citrate drop, the increase in OAA (or pyruvate) signal we observed in the vitreous could relate to this process. Finally, stable and physiological glucose concentration[28] were observed in the vitreous (~4 mM).

## Lipid Synthesis Does Not Account for the Vitreous Citrate Decrease at the Onset of RGC Maturation

Citrate is a well-known substrate for lipid biosynthesis, catalyzed by the ATP-citrate lyase enzyme (ACLY). To test whether the measured drop of citrate might be the result of an increase in lipid synthesis in the retina, we determined the relative lipid composition of the chloroform phase of retinal extracts with particular attention to steroid content, fatty acyl number and poly- or monounsaturations (Supplementary Fig. S2). Seven identifiable lipid resonances were analyzed relative to the total amount of fatty acids (free fatty acids and fatty acyls: methyl peak at 0.88 ppm) (Supplementary Fig. S2B). The following observations were made: (1) no differences in relative fatty acyl chain unsaturation degree occurred from E6 to E8 in the chick and pigeon retina; (2) relative cholesterol content

Investigative Ophthalmology & Visual Science

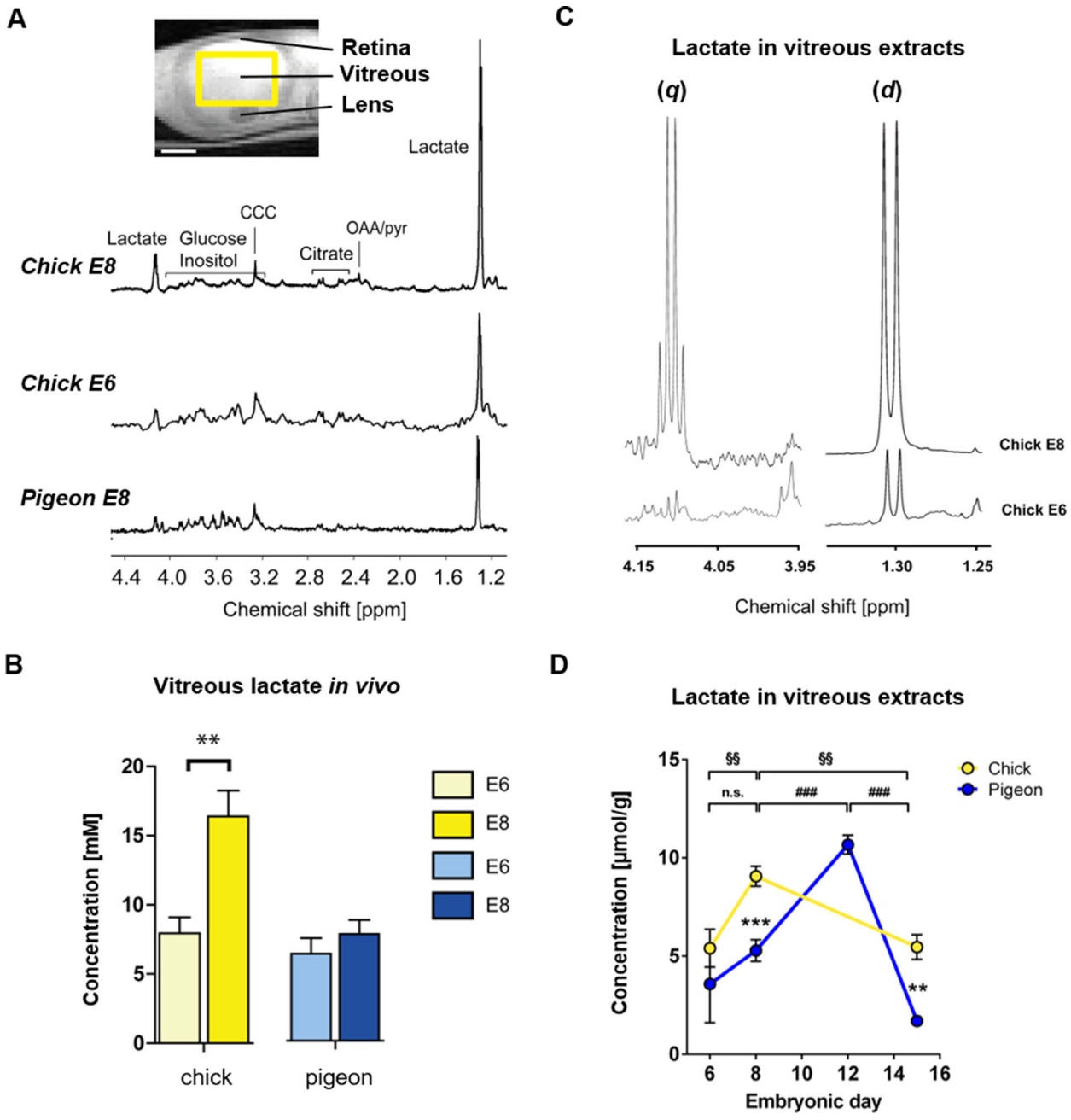


**Figure 3.** A transient net accumulation of vitreous lactate marks the appearance of a retina metabolic switch, with a delayed onset in the pigeon. (**A**, *top*) T2-weighted magnetic resonance image of a chick eye at embryonic stage E8 with position of the VOI (*yellow rectangle*) for in vivo $^{1}$H-MRS. *Scale bar*: 2 mm. (**A**, *bottom*) Localized in vivo $^{1}$H-MRS spectra of the vitreous of chick at E8 and E6, as well as in pigeon at E8. CCC, choline containing compounds; OAA/pyr, oxaloacetate or pyruvate. (**B**) Quantification of lactate in the spectra in vivo (paired Student's *t*-test; $^{**}P < 0.005$; $n = 5$–6 per group). (**C**) Doublet (d) and quadruplet (q) resonances of lactate in $^{1}$H-NMR spectra of vitreous metabolite extracts from chick at E8 and E6. (**D**) Quantification of the high-resolution $^{1}$H-NMR spectra of vitreous extracts reveal an increase in lactate between E6 and E8 in chick ($^{\$\$}P < 0.01$) and between E8 and E12 in pigeon ($^{\#\#\#}P < 0.0005$). This rise in lactate occurred with a delay of 3 days, as revealed by the higher concentration in chick compared with pigeon at E6 ($^{***}P < 0.0005$), and was transient in nature as revealed by the drop occurring in chick from E8 to E15 ($^{\$\$}P < 0.01$) and pigeon from E12 to E15 ($^{\#\#\#}P < 0.0005$). Finally, at E15, piegon had lower levels of lactate than chick ($^{**}P < 0.01$). Unpaired Student's *t*-test, $n = 6$ to 7 chicks and $n = 4$ to 7 pigeons per groups. All data are presented as mean ± SEM.

(0.68 ppm) and mono- and polyunsaturated fatty acids (2.80 and 5.30 ppm) increased from E6 to E8 in both the chick and pigeon (Supplementary Figs. S2A, S2C, S2D); and (3) only in the pigeon retina was there an increase in triglyceride (4.15 and 5.20 ppm) and phospholipid (4.00 ppm) content relative to total fatty acids (Supplementary Fig. S2D). These differences in lipid composition between E6 and E8 were more pronounced in the pigeon than in the chick, an indication that citrate is not the major source for lipid biosynthesis. Together these results indicate that citrate consumption is unlikely to drive fatty acid or cholesterol synthesis.

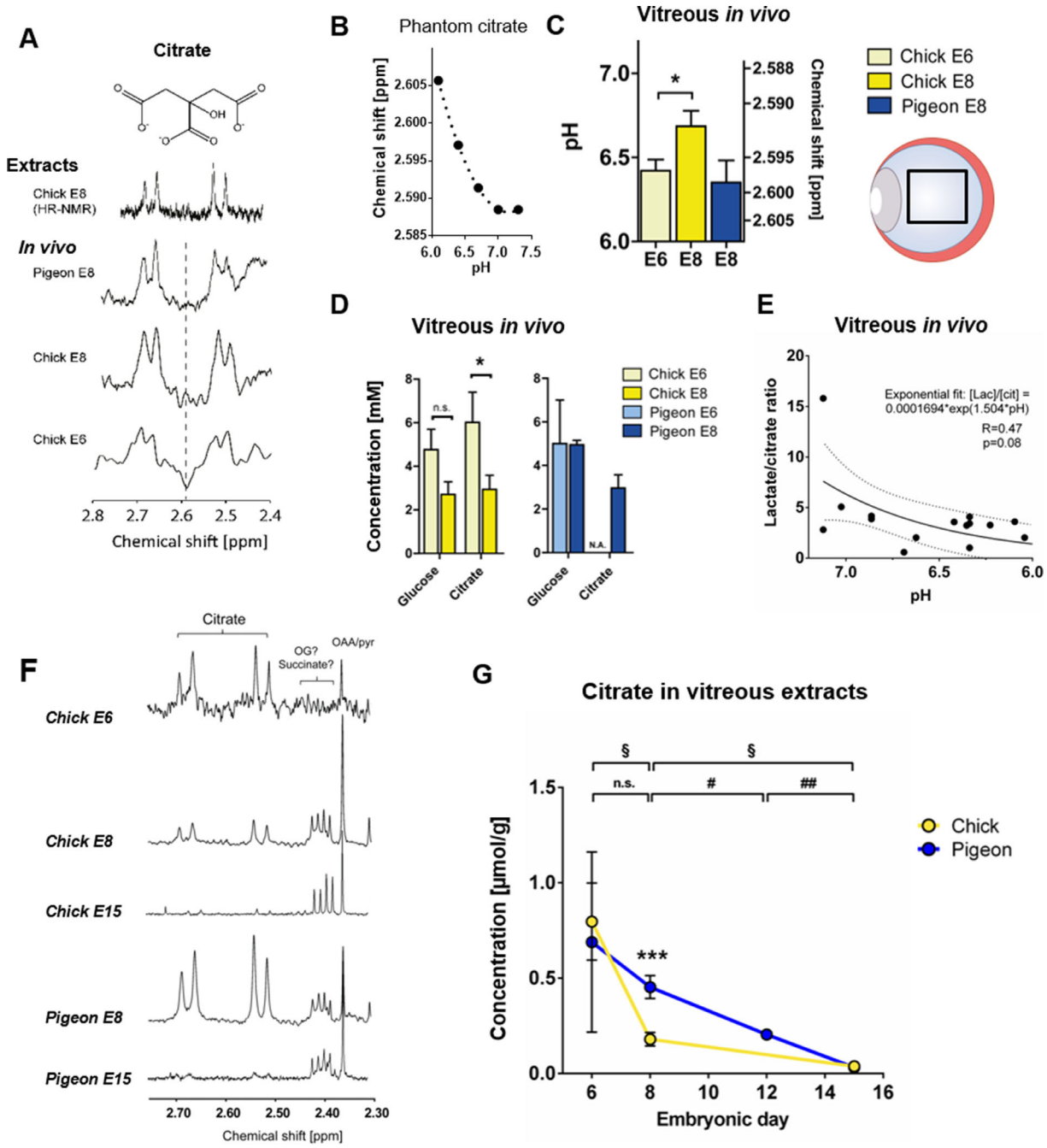


**Figure 4.** A decrease in vitreous citrate parallels lactate and pH increases as the retina undergoes a metabolic switch. (**A**) The pH-dependent chemical shift of citrate at 2.60 ppm was identified in the vitreous of bird embryo in vivo and confirmed in vitro. (**B**) pH-dependence of citrate chemical shift around physiological values as measured in vitro (phantoms). (**C**) In vivo pH measurement in vitreous (paired Student's *t*-test; $^{*}P < 0.05$; $n = 5$–6 per group). (**D**) Quantification of in vivo $^{1}$H-MRS spectra from chick and pigeon vitreous (paired Student's *t*-test; $^{*}P < 0.05$; n.s.; $n = 5$–6 per group; N.A. refers to unquantifiable metabolite). (**E**) Relation between vitreous pH and lactate-to-citrate ratio. (**F**) Typical in vitro $^{1}$H-NMR spectra of extracted metabolites from vitreous of chick at E15, E8, E6 and pigeon at E8 and E15 showing the citrate resonances relative to the OAA/pyr peak (OAA/pyr: oxaloacetate or pyruvate; OG: oxoglutarate). (**G**) Quantification of citrate from $^{1}$H-NMR spectra of metabolite extracts from the vitreous of chick and pigeon (chick vs. pigeon, $^{***}P < 0.0005$; chick, $^{\S}P < 0.05$; pigeon, $^{\#}P < 0.05$, $^{\#\#}P < 0.005$; unpaired Student's *t*-test; $n = 4$–7 per group). All data are presented as mean ± SEM.

## Temporal Modulation of Glycolysis Regulator Expression in the Retina Suggests That the Nature of the Metabolic Switch is Glycolytic

Finally, we analyzed the expression of mRNA transcripts for key enzymes controlling the metabolic pathways of lactate and citrate metabolism using RT-qPCR in the isolated retina (Fig. 5A). The results indicate that: (1) gene expression of the rate limiting glycolytic enzyme PFK1 did not change during the metabolic switch window considered (i.e., E6–E8 for chick and E8–E12 for pigeon), however, its allosteric activator, the enzyme PFK2, also called 6-phosphofructo-

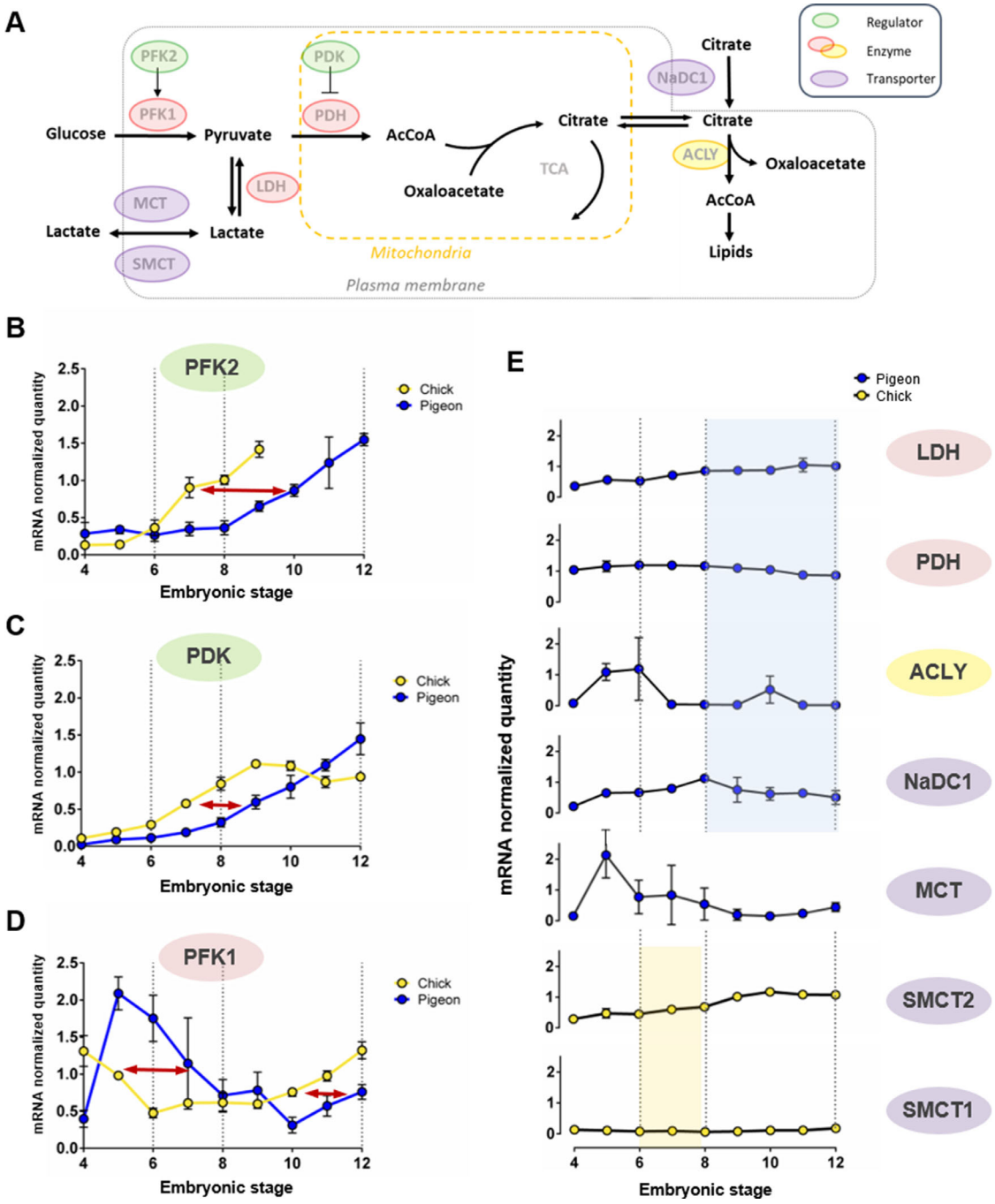


**Figure 5.** Temporal modulation of glycolysis regulator expression in the retina suggests that the nature of the metabolic switch is glycolytic. (**A**) Schematic representation of main metabolic pathways involved in the metabolic switch AcCoA: Acetyl Coenzyme A. (**B–D**) Delayed relative mRNA expression of glycolytic switch regulators between pigeon and chick during retina development. The *red arrow* highlights the delay. (**B**) PFK2 expression is increased over time (time effect: $F_{8,36} = 30.98$, $P < 0.0001$) and delayed by ~3 days between species (interaction: $F_{8,36} = 11.33$, $P < 0.0001$; 2-way ANOVA). (**C**) PDK expression is increased over time (time effect: $F_{8,36} = 28.01$, $P < 0.0001$) and delayed by ~2 days between species (interaction: $F_{8,36} = 165.4$, $P < 0.0001$; 2-way ANOVA). (**D**) PFK1 expression is increased over time (time effect: $F_{8,36} = 20.17$, $P < 0.0001$) and delayed by ~2 to 3 days between species (interaction: $F_{8,36} = 12.58$, $P < 0.0001$; 2-way ANOVA). (**E**) Time-dependent gene expression of remaining enzymes in the retina during the time windows considered for the metabolic switch in chick (E6 vs. E8; *yellow shading*) and pigeon (E8 vs. E12; *blue shading*). Relative mRNA expression shows modest differences in PDH (–26%; $P = 0.0006$) and NaDC1 (–55%; $P = 0.01$), and no difference for LDH, ACLY, and MCT (n.s.) for pigeon enzymes (unpaired Student's *t*-test between E8 and E12), and a strong increase in SMCT2 (+72%; $P < 0.0001$) but not SMCT1 (n.s.) for chick enzymes (unpaired Student's *t*-test between E6 and E8). At each developmental stage, data are from three biological replicates, including 3 to 10 retinas, and presented as mean ± SD.

Investigative Ophthalmology & Visual Science

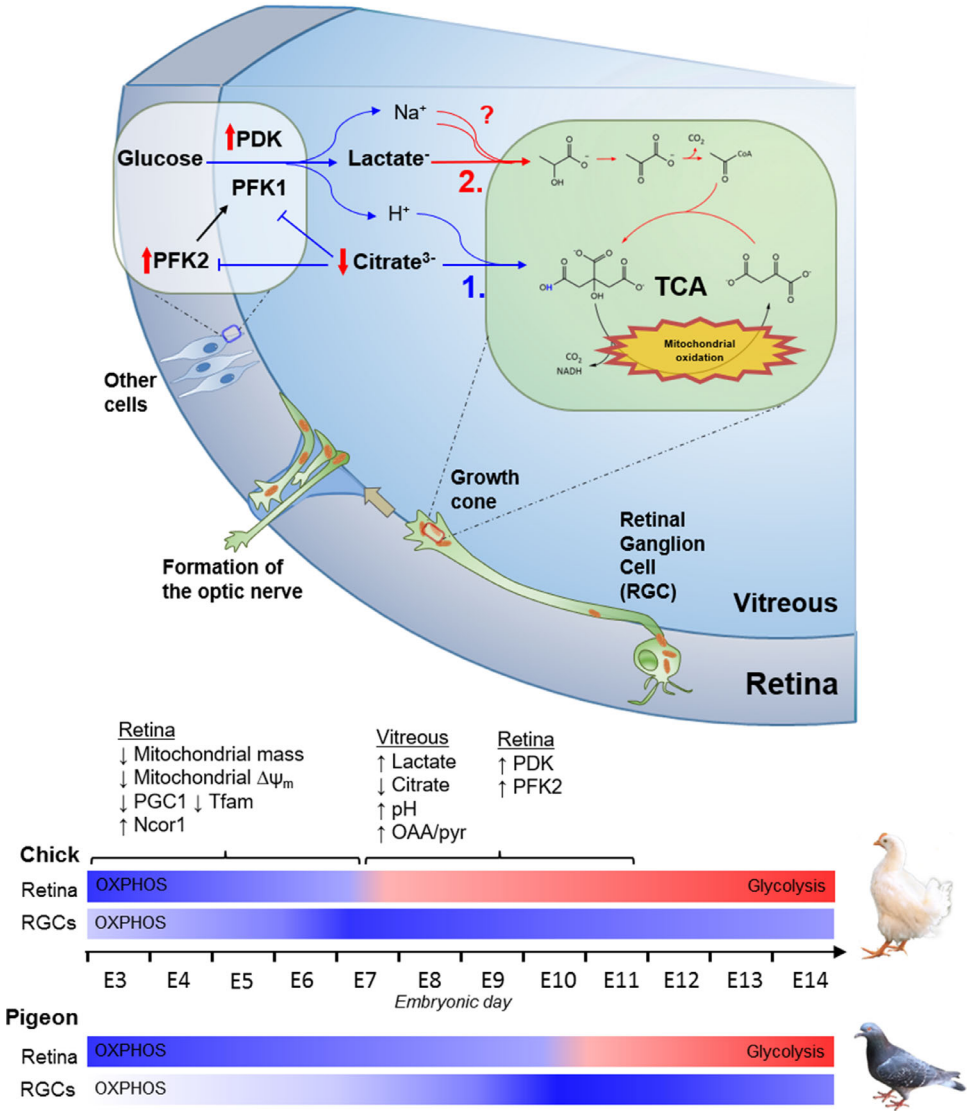


**Figure 6.** Proposed model of neuroenergetic metabolic switch associated with RGC growth and axogenesis. We propose that citrate in the vicinity of oxidative RGCs and their expanding axons/growth cones serves as a rapid and available energy substrate through their TCA cycle (1. *blue arrows*). In this early stage, high citrate concentration prevents aerobic glycolysis in surrounding cells by inhibiting PFK. Through the course of RGC growth, citrate oxidation and removal from the vitreous leads to a rise in vitreous pH. The two-fold vitreous [$H^+$] decrease favors the two-fold lactate increase from retina glycolytic activity (regulated by PDK and PFK expression levels) through MCT lactate/$H^+$ cotransport and SMCT lactate/$Na^+$ cotransport. The transient lactate accumulation in the vitreous could serve as a new mitochondrial carbon substrate (2. *red arrows*), prevent an excessive rise in pH induced by citrate oxidation, reduce oxygen consumption in the outer retina to maintain a sufficient pO2 level in the vitreous, or serve as a metabolic signaling role associated with RGC axonal outgrowth.

2-kinase/fructose-2,6-bisphosphatase, showed an approximate four-fold increase in expression of the isoenzyme 3 at the end of the switch (Fig. 5B); (2) pyruvate dehydrogenase (PDH) mRNA levels remained constant throughout the switch but its inhibitor, PDK, was upregulated (Fig. 5C). These results strongly indicate that the retina undergoes metabolic remodeling toward aerobic glycolysis; (3) this reprogramming most likely leads to the cellular release of lactate, via $H^+$-coupled or $Na^+$-coupled monocarboxylate transporters (MCTs or SMCTs), through the activity of LDH all of which are expressed during the glycolytic switch time window (Fig. 5E); (4) citrate plasma membrane transporter (NaDC1) expression decreased during the switch, whereas ACLY was poorly expressed (Fig. 5E), in line with the utilization of citrate for oxidation rather than lipid biogenesis; and (5) a delay of 3 days was observed between the slopes of the time-dependent PFK2 (interaction: $P < 0.0001$, 2-way ANOVA; Fig. 5B), and PDK (interaction: $P < 0.0001$, 2-way ANOVA; Fig. 5C) expression levels in the chick and pigeon, reconfirming the link between the metabolic switch and retinal neurogenesis. Of note, a peak in PFK1 (Fig. 5D) was observed before the switch, at the time of high mitochondrial content and activity (i.e., ~E5 for the pigeon and ~E3 for the chick) with a ~2-day delay, potentially stimulating glycolysis to match mitochondrial pyruvate needs.

When all of these data are considered, an integrative picture that emerges is an interlocking regulatory cascade shared between two neighboring compartments of the embryonic avian eye that links lactate and citrate levels to PFK and PDK orchestrating aerobic glycolysis (Fig. 6).

Investigative Ophthalmology & Visual Science

## Discussion

In this study, we used high-field and high-resolution $^{1}$H-MRS of the whole eye or its parts, in vivo, and of isolated tissue extracts to investigate for metabolic remodeling during retina neurogenesis. We report the appearance of a metabolic switch that is tightly related to neuronal differentiation in the avian retina in vivo, leading to a cell-type-specific imbalance between aerobic glycolysis and oxidative phosphorylation, translating into metabolite exchanges between retina and vitreous body.

### Mitochondria Characterization

Early studies have suggested that the inner layers of the adult avian retina possess little mitochondrial activity,[29] compatible with its high glycolytic activity. This metabolic specificity has been later shown to have a developmental origin.[6,7] Accordingly, we found that mitochondria number per cell gradually decreased between E3 and E10 in chick and pigeon retinas (Fig. 1). The idea that mitochondria play an important role in retinal progenitor cells is also supported by the high expression of mitochondria biogenesis genes at early stages. Conversely, the observed gradual decreased expression of these genes in differentiating cells suggests that postmitotic cells have lower mitochondrial requirements. Current knowledge suggests that proliferating cells rely mainly on glycolysis to produce their energy, whereas on differentiation they switch to oxidative phosphorylation for increased efficiency and reduced biosynthesis.[30] Although the high content of active mitochondria found in uncommitted retinal progenitor cells does not exclude glycolytic activity, our results suggest higher oxidative capacity than previously thought during cell proliferation.

Interestingly, in the pigeon, the drop of mitochondrial activity and cell differentiation were similarly delayed. This species-specific timing strongly suggests that metabolic remodeling is associated with the onset of neurogenesis. It is striking that RGCs, whose genesis peaks at E6, maintain a high content of active mitochondria that characterizes early progenitor, whereas the other retinal cells display reduced mitochondria content and activity. The unique high oxidative capacity of RGCs likely reflects their particularly high metabolic requirements; and RGC axogenesis probably underlies this energetic remodeling, as illustrated by the high mitochondrial migration following the growth cone (Fig. 1).

### Transient Net Lactate Accumulation is Specific to the Vitreous

Mitochondrial remodeling was associated with a transient vitreous lactate accumulation (Figs. 2, 3) that matched the delayed neurogenesis in the pigeon, and correlated with the upregulation of glycolysis genes in the chick and pigeon retina, a strong argument in favor of a retinal origin of lactate (Fig. 5). The cellular expression of PFK2, together with PDK, provides an efficient way of blocking pyruvate entry in mitochondria, leading to significant lactate production and release. This phenomenon is typically observed in cancer cells with high glycolytic activity.[31] Although the contribution of other surrounding glycolytic tissues in the avian eye, that is, the inner limiting membrane[32] or the lens[33] cannot be excluded, they develop at the same rate in both the chick and pigeon, and hence are unlikely to account for the delayed lactate secretion observed in the pigeon. Furthermore, mitochondrial loss in the lens has been shown to occur relatively late, that is, only from E8 in the chick,[34] in line with the slower lactate increase measured in this tissue (Supplementary Fig. S1D). Future studies will identify which type of retinal cells are predominantly responsible for the rise in glycolysis regulator expression and high lactate production and release in the vitreous. Interestingly, lactate release in the vitreous was not associated with a drop in pH, as would be expected from $H^+$-coupled lactate transport (through MCT) but coincided with pH increase. This can be explained by the presence of $Na^+$-coupled lactate transporter (SMCT2 in particular) expression, providing a mechanistic link to understand lactate flux directionality.

### Citrate Oxidation Drives the Glycolytic Switch

Vitreous citrate appears to be a trigger for the appearance of the glycolytic switch and metabolite fluxes at the retinal-vitreous interface that would serve a developmental function (Fig. 6). Citrate is a well-known inhibitor of PFK1 and PFK2,[35–38] and lower levels of vitreous citrate are likely to provide a favorable environment for surrounding glycolytic retinal cells. Citrate is an important intermediate of the tricarboxylic acid (TCA) cycle in mitochondria, in which its oxidation leads to cellular ATP production. The detection of the citrate/$Na^+$ plasma membrane cotransporter NaDC1 in the retina (Fig. 5E) suggests that citrate is taken up by retinal cells.[39] The function of vitreous citrate appears to serve a nutritive role for mitochondrial ATP production, more so than one linked to lipid biosynthesis (Supplementary Fig. S2). The similar retinal lipidic profile between the two species together with the levels of lipogenic enzyme ACLY, at the limit of detection, suggest that lipid supply for axogenesis might arise solely from transport and mobilization from yolk sac storage.[40,41] The abundance of active (MitoDsRed2-labeled) mitochondria in newborn RGCs, in which they are rapidly translocated in growing axons (Figs. 1E–J), suggest that citrate might fuel axogenesis.

Kanow et al.[42] have recently described a mechanism in the vascularized mouse retina, in which lactate is secreted by glycolytic photoreceptors to inhibit retinal pigment epithelium cells, enabling glucose to reach the inner layers of the retina.[42] A similar nutrient-saving mechanism may be operative in the avian retina, in which the glycolytic switch in the non-RGCs could spare blood-borne oxygen to maintain $pO_2$ levels in the vitreous for the mitochondria-rich RGC axons. It is plausible that citrate and lactate, when concentrated in the vitreous, provide trophic support alternatively for the highly oxidative RGCs undergoing axonal growth. Neurons are well known to take up and oxidize lactate under normal glucose supply.[43] Glial cells have been shown to release lactate and citrate that can serve as oxidative support for surrounding neurons in the adult brain and retina.[44–47] Interestingly, the contribution of retinal glial cells here is minimal because the Müller cells are the last cell type to appear during retinal neurogenesis,[48,49] and are not yet born at the embryonic stages investigated in the present study. Our results show the presence of both $H^+$- and $Na^+$-coupled MCT expression in the retina, which could be implicated in the neuronal lactate uptake. Even though our results indicate lower expression of the neuron-specific lactate transporter SMCT1 compared with SMCT2, its higher affinity could compensate for the putative lower enzyme level.[50] Although cell specific contributions for the observed

Investigative Ophthalmology & Visual Science

redistribution of metabolite content remains to be identified, we speculate that given the high mitochondria reliance of RGC during the metabolic switch, vitreous citrate and lactate consecutively provide oxidizable fuel for axogenesis. Nevertheless, besides their role as neuroenergetic substrate, citrate and lactate both could participate in the process involved in neurogenesis, for example intracellular pH changes; histone acetylation by citrate; signaling through lactate receptors; or diffusion of morphogens.[51–54]

### Interspecies Disparities

Like the avian retina, retinal progenitor cells in the mouse retina have a high density of mitochondria. Esteban-Martínez et al.[55] have shown that cell differentiation into RGCs elicits mitophagy and a glycolytic switch, however, the relative mitochondrial content in RGC axons were not assessed.[55] Our data show no evidence for mitophagy and mitochondrial elimination from RGC in the avian retina, pointing toward cell division and axonal recruitment as a primary event accounting for mitochondria dilution in proliferating retinal progenitors. Unlike rodents and birds, *Xenopus* retinal progenitor cells strongly depend on glycolysis for proliferation and biosynthesis, but can switch to oxidative phosphorylation when RGCs differentiate.[56] These interspecies disparities might be intrinsic to each eye morphology, relative cell populations, and the local microenvironment experienced by the growing neurons during embryogenesis.[57] For instance, the pecten oculi lying at the inner retinal-vitreous interface in avian tissue is a potential source of nutrients and oxygen to the inner retinal layers, compensating for the lack of vascularization in this species.[58] Although vascularization of the pecten oculi occurs only several days after the glycolytic switch reported here, its onset has been shown to appear with a 3-day delay between chick and pigeon as well,[59] suggesting that retinal neurogenesis might be adapted to the evolution of the eye's physiology in a species-dependent manner. Interestingly, the vascularized primate retina displays virtually no vascularization in the central fovea, a region with the highest RGC density, and so metabolism there might be subjected to similar metabolic adaptations as those operating in the embryonic bird retina. Given that bird retinas recapitulate key features of the human fovea and macula, that is, high density of RGCs, high ratio of RGC to photoreceptors, and prevalence of cones over rods,[12,60] avian eye models hold an important place clinically toward understanding diseases of the human eye that affect high visual acuity.

## Conclusions

The findings presented in this study identify vitreous citrate oxidation and retinal lactate release, measured in ovo, as potential mechanisms that assist retinal RGC development associated with high-acuity vision, and illustrate how neurogenesis can remodel neuroenergetics.

### *Acknowledgments*

The authors thank Philippe Delaunay for the supply of pigeon eggs, Lidia Matter-Sadzinski for her critical reading of the manuscript, Katarzyna Pierzchala for her help with metabolite extraction, and Faezeh Sanaei Nezhad for her advice and help in metabolite quantifications using the jMRUI software routine. PCR and RT-qPCR experiments were performed at the iGE3 genomics platform of the University of Geneva (https://ige3.genomics.unige.ch/index.php).

Supported by the Swiss National Science Foundation (Grant 31003A-149458, JMM), the Gelbert Foundation (JMM), and the Canton of Geneva. Experiments were also supported by the Center for Biomedical Imaging of the University of Lausanne, University of Geneva, Geneva University Hospital, Lausanne University Hospital, Swiss Federal Institute of Technology, and the Leenaards and Louis-Jeantet Foundations. The authors alone are responsible for the content and writing of the article.

Disclosure: **A. Cherix,** None; **L. Brodier,** None; **C. Poitry-Yamate,** None; **J.-M. Matter,** None; **R. Gruetter,** None

### *References*

1. Ferreira LMR. Cancer metabolism: the Warburg effect today. *Exp Mol Pathol*. 2010;89:372–380.
2. Koppenol WH, Bounds PL, Dang CV. Otto Warburg's contributions to current concepts of cancer metabolism. *Nat Rev Cancer*. 2011;11:325–337.
3. Warburg O. Über den stoffwechsel der carcinomzelle. *Naturwissenschaften*. 1924;12:1131–1137.
4. Jones W, Bianchi K. Aerobic glycolysis: beyond proliferation. *Front Immunol*. 2015;6:1–5.
5. Krebs HA. Über den stoffwechsel der netzhaut. *Biochem Z*. 1927;189:57–99.
6. Buono RJ, Sheffield JB. Changes in expression and distribution of lactate dehydrogenase isoenzymes in the developing chick retina. *Exp Eye Res*. 1991;53:199–204.
7. Buono RJ, Sheffield JB. Changes in distribution of mitochondria in the developing chick retina. *Exp Eye Res*. 1991;53:187–198.
8. Li Y, Sheffield JB. An immunohistochemical analysis of hypoxia in multi-layer avascular retina and vascular pecten oculi of the developing chicken. *Med Res Arch*. 2016;3:1–23.
9. Snow RL, Robson JA. Ganglion cell neurogenesis, migration and early differentiation in the chick retina. *Neuroscience*. 1994;58:399–409.
10. Boss A, Oppitz M, Wehrl HF, et al. Measurement of T1, T2, and magnetization transfer properties during embryonic development at 7 Tesla using the chicken model. *J Magn Reson Imaging*. 2008;28:1510–1514.
11. Bain MM, Fagan AJ, Mullin JM, McNaught I, McLean J, Condon B. Noninvasive monitoring of chick development in ovo using a 7T MRI system from day 12 of incubation through to hatching. *J Magn Reson Imaging*. 2007;26:198–201.
12. Rodrigues T, Krawczyk M, Skowronska-Krawczyk D, Matter-Sadzinski L, Matter J-M. Delayed neurogenesis with respect to eye growth shapes the pigeon retina for high visual acuity. *Development*. 2016;143:4701–4712.
13. Zeevalk GD, Nicklas WJ. Lactate prevents the alterations in tissue amino acids, decline in ATP, and cell damage due to aglycemia in retina. *J Neurochem*. 2000;75:1027–1034.
14. Hamburger V, Hamilton HL. A series of normal stages in the development of the chick embryo. 1951. *Dev Dyn*. 1992;195:231–272.
15. Kiyama T, Chen C-K, Wang SW, et al. Essential roles of mitochondrial biogenesis regulator Nrf1 in retinal development and homeostasis. *Mol Neurodegener*. 2018;13:56.
16. Beckervordersandforth R, Ebert B, Schäffner I, et al. Role of mitochondrial metabolism in the control of early lineage progression and aging phenotypes in adult hippocampal neurogenesis. *Neuron*. 2017;93:1518.

17. Lima TI, Valentim RR, Araújo HN, et al. Role of NCoR1 in mitochondrial function and energy metabolism. *Cell Biol Int*. 2018;42:734–741.
18. Novak I, Kirkin V, McEwan DG, et al. Nix is a selective autophagy receptor for mitochondrial clearance. *EMBO Rep*. 2010;11:45–51.
19. Chiodini F, Matter-Sadzinski L, Rodrigues T, et al. A positive feedback loop between ATOH7 and a notch effector regulates cell-cycle progression and neurogenesis in the retina. *Cell Rep*. 2013;3:796–807.
20. Brodier L, Rodrigues T, Matter-Sadzinski L, Matter J-M. A transient decrease in mitochondrial activity is required to establish the ganglion cell fate in retina adapted for high-acuiy vision. bioRxiv, doi:10.1101/2020.03.23.002998.
21. Manganas LN, Zhang X, Li Y, et al. Magnetic resonance spectroscopy identifies neural progenitor cells in the live human brain. *Science*. 2007;318:980–985.
22. Ramm P, Couillard-Despres S, Plötz S, et al. A nuclear magnetic resonance biomarker for neural progenitor cells: is it all neurogenesis? *Stem Cells*. 2009;27:420–423.
23. Park J-H, Lee H, Makaryus R, et al. Metabolic profiling of dividing cells in live rodent brain by proton magnetic resonance spectroscopy (1HMRS) and LCModel analysis. *PLoS One*. 2014;9:e94755.
24. Foulds WS. Is your vitreous really necessary? The role of the vitreous in the eye with particular reference to retinal attachment, detachment and the mode of action of vitreous substitutes. *Eye*. 1987;1:641–664.
25. De Smet MD, Gad Elkareem AM, Zwinderman AH. The vitreous, the retinal interface in ocular health and disease. *Ophthalmologica*. 2013;230:165–178.
26. Bishop P. The biochemical structure of mammalian vitreous. *Eye*. 1996;10:664–670.
27. Sultan Kedir A, Georg Seland J, Skauge A, Skauge T. Nanoparticles for enhanced oil recovery: influence of pH on aluminum-cross-linked partially hydrolyzed polyacrylamide-investigation by rheology and NMR. *Energy Fuels*. 2014;28:2343–2351.
28. Miya-Coreixas VS, Maggesissi Santos R, Carpi Santos R, Gardino PF, Calaza K. Regulation of GABA content by glucose in the chick retina. *Exp Eye Res*. 2013;115:206–215.
29. Hughes JT, Jerrome D, Krebs HA. Ultrastructure of the avian retina an anatomical study of the retina of the domestic pigeon (*Columba liva*) with particular reference to the distribution of mitochondria. *Exp Eye Res*. 1972;14:189–195.
30. Folmes CDL, Dzeja PP, Nelson TJ, Terzic A. Metabolic plasticity in stem cell homeostasis and differentiation. *Cell Stem Cell*. 2012;11:596–606.
31. Atsumi T, Chesney J, Metz C, et al. High expression of inducible 6-phosphofructo-2-kinase/fructose-2,6-bisphosphatase (iPFK-2; PFKFB3) in human cancers. *Cancer Res*. 2002;62:5881–5887.
32. Halfter W, Deiss S, Schwarz U. The formation of the axonal pattern in the embryonic avian retina. *J Comp Neurol*. 1985;232:466–480.
33. Bassnett S. Intracellular pH regulation in the embryonic chicken lens epithelium. *J Physiol*. 1990;431:445–464.
34. Bassnett S, Beebe DC. Coincident loss of mitchondria and nuclei during lens fiber cell development. *Dev Dyn*. 1992;194:85–93.
35. Pogson C, Randle P. The control of rat-heart phosphofructokinase by citrate and other regulators. *Biochem J*. 1966;100:683–693.
36. Moreno-Sánchez R, Marín-Hernández A, Gallardo-Pérez JC, et al. Phosphofructokinase type 1 kinetics, isoform expression, and gene polymorphisms in cancer cells. *J Cell Biochem*. 2012;113:1692–1703.
37. Iacobazzi V, Infantino V. Citrate–new functions for an old metabolite. *Biol Chem*. 2014;395:387–399.
38. Newsholme EA, Sugden PH, Williams T. Effect of citrate on the activities of 6-phosphofructokinase from nervous and muscle tissues from different animals and its relationships to the regulation of glycolysis. *Biochem J*. 1977;166:123–129.
39. Sun J, Aluvila S, Kotaria R, Mayor JA, Walters DE, Kaplan RS. Mitochondrial and plasma membrane citrate transporters: discovery of selective inhibitors and application to structure/function analysis. *Mol Cell Pharmacol*. 2010;2:101–110.
40. Bauer R, Plieschnig JA, Finkes T, Riegler B, Hermann M, Schneider WJ. The developing chicken yolk sac acquires nutrient transport competence by an orchestrated differentiation process of its endodermal epithelial cells. *J Biol Chem*. 2013;288:1088–1098.
41. Yadgary L, Cahaner A, Kedar O, Uni Z. Yolk sac nutrient composition and fat uptake in late-term embryos in eggs from young and old broiler breeder hens. *Poult Sci*. 2010;89:2441–2452.
42. Kanow MA, Giarmarco MM, Jankowski CS, et al. Biochemical adaptations of the retina and retinal pigment epithelium support a metabolic ecosystem in the vertebrate eye. *Elife*. 2017;6:1–25.
43. Larrabee MG. Lactate uptake and release in the presence of glucose by sympathetic ganglia of chicken embryos and by neuronal and nonneuronal cultures prepared from these ganglia. *J Neurochem*. 1983;40:1237–1250.
44. Poitry-Yamate CL, Poitry S, Tsacopoulos M. Lactate released by Müller glial cells is metabolized by photoreceptors from mammalian retina. *J Neurosci*. 1995;15:5179–5191.
45. Pellerin L, Magistretti PJ. Glutamate uptake into astrocytes stimulates aerobic glycolysis: a mechanism coupling neuronal activity to glucose utilization. *Proc Natl Acad Sci U S A*. 1994;91:10625–10629.
46. Mächler P, Wyss MT, Elsayed M, et al. In vivo evidence for a lactate gradient from astrocytes to neurons. *Cell Metab*. 2016;23:94–102.
47. Sonnewald U, Westergaard N, Krane J, Unsgård G, Petersen SB, Schousboe A. First direct demonstration of preferential release of citrate from astrocytes using [13C]NMR spectroscopy of cultured neurons and astrocytes. *Neurosci Lett*. 1991;128:235–239.
48. Tao C, Zhang X. Development of astrocytes in the vertebrate eye. *Dev Dyn*. 2014;243:1501–1510.
49. Doh S, Hao H, Loh SC, et al. Analysis of retinal cell development in chick embryo by immunohistochemistry and in ovo electroporation techniques. *BMC Dev Biol*. 2010;10:8.
50. Srinivas SR, Gopal E, Zhuang L, et al. Cloning and functional identification of slc5a12 as a sodium-coupled low-affinity transporter for monocarboxylates (SMCT2). *Biochem J*. 2005;392:655–664.
51. Tatapudy S, Aloisio F, Barber D, Nystul T. Cell fate decisions: emerging roles for metabolic signals and cell morphology. *EMBO Rep*. 2017;18:2105–2118.
52. Kolko M, Vosborg F, Henriksen UL, et al. Lactate transport and receptor actions in retina: potential roles in retinal function and disease. *Neurochem Res*. 2016;41:1229–1236.
53. Crick F. Diffusion in embryogenesis. *Nature*. 1970;225:420–422.
54. Miyazawa H, Aulehla A. Revisiting the role of metabolism during development. *Development*. 2018;145:dev131110.
55. Esteban-Martínez L, Sierra-Filardi E, McGreal RS, et al. Programmed mitophagy is essential for the glycolytic switch during cell differentiation. *EMBO J*. 2017;36:1688–1706.


Investigative Ophthalmology & Visual Science

56. Agathocleous M, Love NK, Randlett O, et al. Metabolic differentiation in the embryonic retina. *Nat Cell Biol*. 2012;14:859–864.
57. Masland RH. The fundamental plan of the retina. *Nat Neurosci*. 2001;4:877–886.
58. Brach V. The functional significance of the avian pecten: a review. *Condor*. 1977;79:321.
59. Parducci F, Micali A, La Fauci MA, Puzzolo D. [Comparative embryogenesis of the pecten oculi in chickens and pigeons]. *Arch Ital Anat Embriol*. 1987;92:145–158.
60. da Silva S, Cepko CL. Fgf8 expression and degradation of retinoic acid are required for patterning a high-acuity area in the retina. *Dev Cell*. 2017;42:68–81. e6.

Investigative Ophthalmology & Visual Science